Kraft cooking of birch wood chips: Differences between the dissolved organic material in pore and bulk liquor

Wood Chemistry

Linus Kron, Carolina Marion de Godoy, Merima Hasani* and Hans Theliander

Kraft cooking of birch wood chips: differences between the dissolved organic material in pore and bulk liquor

https://doi.org/10.1515/hf-2023-0018
Received February 24, 2023; accepted June 13, 2023;
published online July 7, 2023

Abstract: The delignification of birch chips during kraft pulping was investigated, targeting both the impregnation and cooking steps. Wood chips were impregnated using white liquor, white liquor + NaCl, water or NaCl aqueous solution. Then, the chips were cooked in batch autoclaves applying the same constant composition cooking conditions for all samples. Pulp and two fractions of black liquor (bulk liquor and centrifuged liquor representing the liquor inside the wood chips and fibers) were collected after different pulping times and analyzed for lignin and carbohydrate content. The dissolved wood components were precipitated from selected samples and characterized with respect to composition, molecular weight distribution and structural motifs. Cooking chemicals in the impregnation liquors led to faster delignification and xylan removal during cooking. Higher contents of lignin and xylan were measured in the lumen than in the bulk. The concentration profiles also showed accumulation of dissolved material in the lumen over time, suggesting significant mass transport limitation from lumen to bulk. Further analysis revealed higher fragmentation/degradation of dissolved material with increasing pulping time and in the bulk when compared to the lumen liquor, as demonstrated by the lower molecular weights and the changes in chemical shifts in the NMR spectra.

Keywords: black liquor; hardwood; impregnation; kraft delignification; mass transport

Linus Kron and Carolina Marion de Godoy shared first authorship.

This article is a special contribution associated to a presentation made in the 16th European Workshop on Lignocellulosics and Pulp (EWLP) 2022, Gothenburg, Sweden, Jun 28 to Jul 1, 2022.

***Corresponding author: Merima Hasani**, Division of Forest Products and Chemical Engineering, Department of Chemistry and Chemical Engineering, Chalmers University of Technology, Chalmersplatsen 4, 412 96 Gothenburg, Sweden; and Wallenberg Wood Science Center, Chalmers University of Technology, 412 96 Gothenburg, Sweden, E-mail: merima.hasani@chalmers.se
Linus Kron and Carolina Marion de Godoy, Division of Forest Products and Chemical Engineering, Department of Chemistry and Chemical Engineering, Chalmers University of Technology, Chalmersplatsen 4, 412 96 Gothenburg, Sweden, E-mail: linus.kron@chalmers.se (L. Kron), godoy@chalmers.se (C. Marion de Godoy). https://orcid.org/0000-0003-3510-9826 (L. Kron). https://orcid.org/0000-0003-4143-4801 (C. Marion de Godoy)
Hans Theliander, Division of Forest Products and Chemical Engineering, Department of Chemistry and Chemical Engineering, Chalmers University of Technology, Chalmersplatsen 4, 412 96 Gothenburg, Sweden; and Wallenberg Wood Science Center, Chalmers University of Technology, 412 96 Gothenburg, Sweden, E-mail: hanst@chalmers.se

1 Introduction

The pulp and paper industry has the potential to be a major player in the change towards a bio-based circular economy. With its currently wide selection of available products, as well as promising new alternatives derived from side streams, it can aid in decreasing the production and consumption of fossil-based material. Yet, like many other large-scale industries, it faces the challenge of an increasing global energy demand and raw material scarcity (Pätäri et al. 2016). There is, thus, an ever-present need for a better understanding of the process, in order to increase efficiency and decrease material use. This is particularly relevant in kraft pulping, as it remains the dominant process in the pulp and paper industry.

Throughout the years, many studies have shown how the yield and pulp quality are affected by pulping conditions (e.g., liquor:wood ratio, H-factor, liquor composition, impregnation strategy, etc.) and raw material characteristics, such as chemical composition and wood morphology (Dang and Nguyen 2008; Hatton 1973; Henriksson et al. 2007; Lindgren and Lindström 1996; Santos et al. 2012; Tavast and Brännvall 2017). Still, thorough descriptions of the pulping process, considering not only the overall delignification kinetics, but also including other phenomena such as dissolution of wood components (e.g., lignin and xylan fragments) and mass transport across the heterogeneous system, remain scarce in the literature.

The mechanisms of the main reactions taking place during pulping have been elucidated (Chakar and Ragauskas 2004; Gellerstedt et al. 2004; Gierer 1980; Santos et al. 2013; Sjöström 1977) and the dissolution, sorption and desorption of wood components have been studied (Brelid et al. 2011; Dang et al. 2013, 2016; Saltberg et al. 2009). However, many of the most commonly used models are based on the assumption that the cleavage of lignin inter-unit bonds is the rate limiting step (Nieminen and Sixta 2012; Rahman et al. 2020), often ignoring other effects in favor of a simpler and less computationally demanding approach. The heterogeneous nature of wood and the mass transport of reactants and dissolved products are even more neglected, although more recently, some authors have tried to account for these phenomena, with varying degrees of complexity (Bijok et al. 2022; Dang and Nguyen 2008; Gilbert et al. 2021; Grénman et al. 2010; Nguyen and Dang 2006; Simão et al. 2011, 2008).

Hence, it seems imperative to further characterize the system undergoing kraft cooking, in order to ensure reasonable assumptions when modelling the process. For instance, recent studies have found large differences in concentrations of wood components and cooking chemicals between the liquor in the bulk and that within wood chips (Brännvall and Rönnols 2021; Gilbert et al. 2021; Pakkanen and Alén 2012; Simão et al. 2011). In addition, the mass transfer resistance in the cell wall has been suggested to also provide a considerable impact on the overall pulping behavior (Brännvall and Rönnols 2021; Mattsson et al. 2017; Mortha et al. 1992). Moreover, among the already scarce number of studies on this topic, many have focused on softwood, thus even less is known regarding hardwoods.

In this context, the delignification behavior of birch is investigated by varying the composition of the liquor applied for impregnation and analyzing fractions of the black liquor at different pulping times, aiming at improving the understanding of the impact of mass transport on kraft pulping. The study is carried out with birch, given its abundance in European forests and the increasing relevance of hardwoods in the context of forest management (Forest Europe 2020). Emphasis is put on characterizing the dissolved wood components with respect to composition, mass distribution and structural motifs.

2 Materials and methods

2.1 Materials

Wood chips of mixed birch (*Betula pendula* and *Betula pubescens*) from industrially cut logs grown in southern Sweden were screened to be free of bark and knots, and with thickness between 2 and 6 mm. The chips were air dried and stored at room temperature, yielding an average dry content of 93 % (w/w).

2.2 Kraft cooking

Initially, approximately 25 g of chips were impregnated in 1.5 L autoclaves containing 250 g of one of the four impregnation liquors shown in Table 1. The liquors were chosen to compare the transport of ions via advection and diffusion (impregnating with white liquor) to transport via diffusion only (impregnating with water). Furthermore, the effect of addition of sodium ions in either of the cases was studied. The impregnation was carried out at room temperature: Each vessel was loaded with chips and impregnation liquor, deaerated and left under vacuum for 5 min, and then pressurized with nitrogen (5 bar/15 min), according to the procedure of Bogren (2008). Afterwards, the impregnation liquor was removed, and 500 g of fresh cooking liquor, corresponding to liquor WL in Table 1, was added. The high liquor:wood ratio was chosen to ensure an excess of cooking chemicals and near constant concentration in all samples throughout pulping. The residual concentration of OH^- in the spent impregnation liquor WL was 0.55 mol/kg liquor.

The autoclaves were placed in a polyethylene glycol bath (160 °C) and heated for different time periods (10, 20, 30, 60, 90 and 120 min). Samples taken after the first two time points (10 and 20 min) were still in the heating up phase, whereas the other four (30, 60, 90 and 120 min) were taken after the final cooking temperature was reached (heating up time inside the autoclaves: approximately 25 min). The temperature profile of the heating up time is given in the Supplementary Material (Supplementary Figure S1).

After termination of the cook, the black liquor was collected via filtration (bulk liquor, BL). The remaining moist solid residue was centrifuged following the procedure described by Brännvall and Rönnols (2021) to separate the liquor still trapped in the pore system of the treated chips (centrifuged liquor, CL). After centrifugation, the solid residue was washed with distilled water, leached in 4 L of distilled water until neutral pH (leaching water was changed every other day) and dried overnight (105 °C).

Table 1: Composition of the impregnation liquors.

Liquor[a]	Conc. OH^- & HS^- (mol/kg liquor)	NaCl addition (mol/kg liquor)	Total Na^+ (mol/kg liquor)
WL	0.60 & 0.15	–	0.75
WLNa	0.60 & 0.15	1.25	2.00
W	–	–	0
WNa	–	2.00	2.00

[a]WL, white liquor; WLNa, white liquor with addition of NaCl; W, water; WNa, water with addition of NaCl.

2.3 Lignin precipitation

Lignin was precipitated from the two fractions of liquor, BL and CL, following the procedure described by Dang et al. (2016), but considering a final pH of 3.0. In short, concentrated sulfuric acid was added to 50 mL of liquor at room temperature until the final pH was reached. The samples were then frozen overnight, thawed, and the precipitated

lignin was collected on glass fiber filters. The material was dried in an oven (40 °C) for three days.

2.4 Klason lignin quantification

Klason lignin content was determined after acid hydrolysis, following a slightly modified version of the procedure described by the National Renewable Energy Laboratory (Sluiter et al. 2012). The detailed procedures used for pulp and black liquor samples are described in the supplementary material. The measured residual standard deviation (RSD) of the analysis was 4.0 %.

2.5 Acid soluble lignin (ASL) measurement

The filtrate solutions obtained after hydrolysis were analyzed at 205 nm using an UV spectrophotometer (Specord 205, Analytik Jena) and 1 cm quartz cuvettes. The ASL content was calculated based on absorbance measurements and considering an absorptivity constant of 110 $dm^3\ g^{-1}\ cm^{-1}$ (Dence 1992). The RSD was 6.2 %.

2.6 Carbohydrate quantification

The carbohydrates were quantified using the filtrate solutions produced after acid hydrolysis. The samples were analyzed via anion exchange chromatography with pulsed amperometric detection (HPAEC-PAD Dionex ICS-5000, Thermo Fisher Scientific). The system was equipped with a gold reference electrode and Dionex CarboPac PA1 columns (a 2 × 50 mm guard column and a 2 × 250 mm analytical column). The elution (dual pump: 0.26 mL/min and 0.13 mL/min) took place at 30 °C for 25 min using H_2O/200 mM NaOH, followed by a washing step of 13 min using 200 mM NaOH/200 mM NaOH + 170 mM sodium acetate. The injection volume was 10 µL. All samples were filtered with 0.2 µm PTFE filters prior to analysis. Data processing was carried out with the Chromeleon software v. 7.1. The detected amounts of sugar monomers were corrected for the yield loss after acid hydrolysis (Wojtasz-Mucha et al. 2017) and expressed as anhydro sugars (Janson 1974). Thus, the reported data is referred to as polysaccharides (e.g., xylan), however without accounting for any substituents. The highest RSD calculated was 3.6 % (for Rhamnan measurements).

2.7 GPC

The molecular weight distribution (MWD) of precipitated lignin samples was measured using gel permeation chromatography (PL-HPC 50 Plus Integrated GPC system, Polymer Laboratories, Varian Inc.). The system used two 300 × 7.5 mm PolarGel-M columns and one 50 × 7.5 mm PolarGel-M guard column. Dimethyl sulphoxide (DMSO) with 10 mM LiBr was used as the mobile phase and the flow rate was 0.5 mL/min at 50 °C. Detection was made using a UV detector operating at 280 nm, as well as a refractive index (RI) detector. Both detectors were calibrated with 10 Pullulan standards ranging from 0.180 to 708 kDa (Varian PL2090-0100, Varian Inc). Samples were dissolved in the mobile phase overnight, diluted to 0.25 mg/mL and filtered with 0.2 µm syringe filters. Each sample was run in duplicate. Analysis of data was made with the Cirrus GPC Software 3.2.

2.8 NMR

The precipitated lignin samples were also analyzed with 2D NMR spectroscopy (heteronuclear single quantum coherence, HSQC). The spectra were recorded at 25 °C using a Bruker Avance III HD (Rheinstetten, Germany) with a 5 mm TXO cold probe operating at 800 and 200 MHz for ^1H and ^{13}C, respectively. The pulse program used was hsqcedetgpsisp2.3 with 96 ms and 6 ms acquisition time for ^1H and ^{13}C, in that order, an FID size of 3072 and 512 points, respectively, and 24 scans with 1 s relaxation time, resulting in an experimental time of 3 h 51 min. Samples were dissolved in deuterated DMSO-d_6 to a concentration of 140 mg/mL. A small fraction could not be dissolved and was separated by centrifugation (12,500 rpm for 5 min). The supernatant was then used for analysis in 3 mm tubes. Data analysis was done in Bruker TopSpin 4.1.4 software.

3 Results and discussion

3.1 Wood composition

The chemical composition of the untreated wood is presented in Table 2. The overall composition of the raw material agreed with what is usually reported for birch wood. The content of Klason lignin was slightly higher than the average found for *B. pendula* (Olm et al. 2009; Pinto et al. 2005; Santos et al. 2011), being closer to results attained with *B. pubescens* (Luostarinen and Hakkarainen 2019; Mulat et al. 2018). Also, the levels of carbohydrates, especially xylan, were somewhat lower than previously reported. A possible reason for the discrepancies could be the presence of extractives, as no extraction was made prior to the measurements. Extractives may co-precipitate with the lignin, thus explaining the high Klason lignin content, as well as hinder the hydrolysis of the polysaccharides (Shin et al. 2004).

Table 2: Composition of birch wood (%, w/w).

Component	$\bar{x} \pm s$
Klason lignin	24.0 ± 1.0
Acid soluble lignin	3.0 ± 0.0
Glucan	38.3 ± 0.1
Xylan	18.4 ± 0.0
Arabinan	0.4 ± 0.0
Galactan	0.7 ± 0.0
Mannan	1.8 ± 0.0

Detected amount: 86.6 ± 1.0 %.

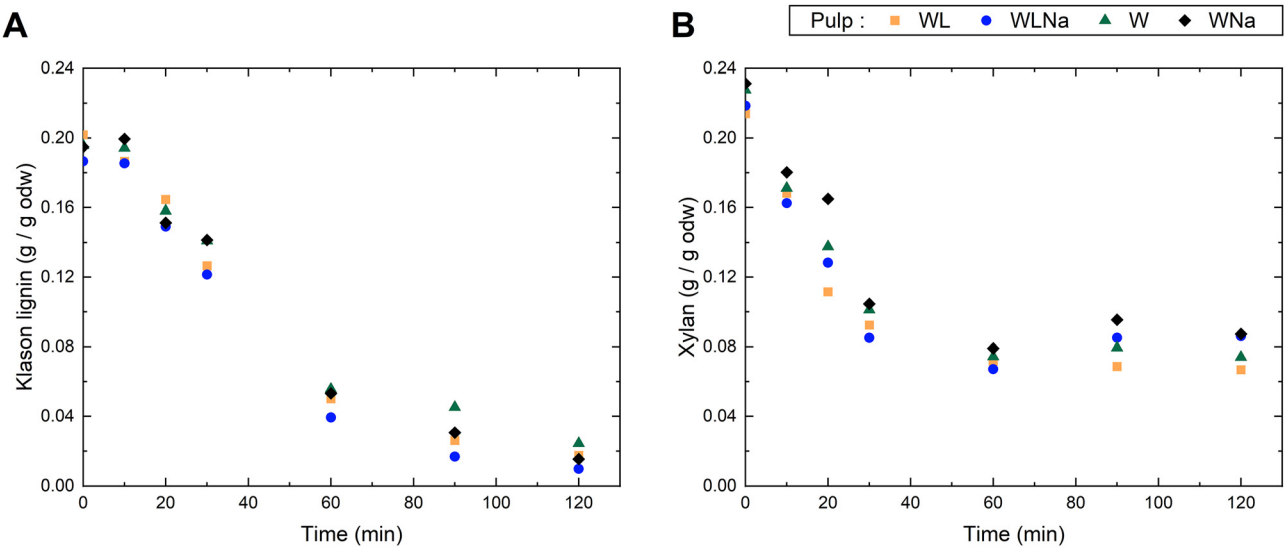

Figure 1: Content of residual Klason lignin (A) and xylan (B) in pulp samples collected throughout cooking. Results in g/g of oven-dried wood (odw). Values at 0 min represent samples of wood chips analyzed after impregnation.

3.2 Effect of the impregnation liquors over pulping

Figure 1A shows the residual Klason lignin content in the pulp versus the cooking time for samples impregnated using different liquors. Similarly, Figure 1B presents the xylan content in the pulps. Although no large differences occurred, samples impregnated with the active ions (liquors WL and WLNa) showed a higher rate of delignification and carbohydrate degradation, when compared to samples impregnated with liquors W and WNa (pure water and NaCl solution, refer to Table 1). This behavior is reasonable and highlights the impact of the transport of cooking chemicals within the wood chips: In wood chips samples impregnated with liquors W and WNa, the active ions that were added in the cooking step had to be transported exclusively via diffusion within the system. Whereas in cases WL and WLNa, some ions had already been transported due to advection during the impregnation phase, resulting in overall faster reactions.

Regarding the conditions with increased sodium concentration during impregnation (samples treated with liquors WLNa and WNa), only a marginal increase in delignification rate was observed when applying the present conditions. Moreover, this difference was only significant between WL and WLNa (at $\alpha = 0.05$), whereas the same could not be seen between W and WNa. A possible explanation for an increase is the Donnan effect (Bogren et al. 2009), which predicts the local concentration of hydroxide ions within the cell wall to be increased in liquors with higher ionic strength, thus increasing the rate of delignification. This observation is different from previously reported effects of inactive ions during cooking (Brännvall and Rönnols 2021; Sixta and Rutkowska 2006), in which the delignification rate was shown to decrease with increasing sodium addition (0–1.7 M NaCl and 0–0.25 M Na_2CO_3, respectively). The decrease in delignification at higher ionic strength has been suggested to result from the decreased solubility of lignin at these conditions (Dang et al. 2013; Saltberg et al. 2009). Estimated from the amount of impregnation liquor remaining in the chips, the corresponding value in the present study is 0.1 M NaCl. It is likely that, by adding extra salt only during impregnation, the final sodium content during pulping was not sufficient to affect lignin solubility and thus the delignification as a whole.

Further analysis of Figure 1A shows that the delignification rate reached a maximum between 30 and 60 min, which coincides with the system achieving the final cooking temperature. After 60 min, the rate decreased, but the lignin content in the pulp continued to decline for the remainder of the cook. In the case of xylan (Figure 1B), the dissolution rate decreased significantly between 30 and 60 min. The early decrease in reaction rate indicates that most xylan is dissolved at relatively low temperatures, which corresponds well with earlier findings (Axelsson et al. 1962). After 60 min, the xylan concentration remained fairly stable, some measurements (e.g., WLNa) even suggested a slight increase in xylan content. A likely explanation for any increase in concentration is the deposition of xylan onto the fibers, however more experiments in this time range would be necessary in order to draw further conclusions about this phenomenon. The stabilization of xylan concentration in the pulp also

hints at the presence of a fraction of xylan that is more resistant to the pulping condition. It has previously been suggested that two different fractions of xylan exist within the cell wall: one having more interaction with lignin, and the other more resistant fraction associated with cellulose instead (Dammström et al. 2009; Ruel et al. 2006).

3.3 Comparison between pulp, BL and CL

The contents of dissolved lignin and xylan in the fractions of liquor are presented in Figure 2. Both curves associated with BL followed a similar, but opposite behavior when compared with pulp. However, due to the small amount of lignin removed from pulp after 60 min, no significant increase in the amount of dissolved Klason lignin was detected in the BL at the end of the process, even though delignification occurred throughout the whole cook (refer to Figure 1A). On the other hand, the profile of the CL data was highly affected by the changes in total dissolution rate from the cell wall, so much so that the lignin content decreased after 60 min, which agrees with the reduced delignification rate at this point.

Further analysis of Figure 2A reveals the differences in concentration of Klason lignin in the two fractions of spent cooking liquor during the pulping process. Independent of impregnation scenario, the concentrations in the centrifuged liquor are substantially higher compared to the bulk. Similar relative differences are found in literature (Pakkanen and Alén 2012; Simão et al. 2011). Furthermore, the shapes of the concentration profiles differ between the two liquors. For the bulk fraction, the concentration of lignin initially increases until a virtual plateau is reached. Whereas for the centrifuged fraction, there is a steep rise in concentration, leading to a maximum (about 2 %, w/w), followed by a gradual decrease. These profiles can be explained by the interplay between the dissolution of lignin and the transport of the lignin fragments within the system. At the beginning of the cook (<60 min), the high delignification rate leads to a quick dissolution of lignin fragments, that are then removed from the cell wall into the lumen. However, the subsequent diffusion of the fragments from the lumen to the bulk liquor appears to be relatively slow when compared to the reaction rate and mass transport in the cell wall, resulting in the sharp increase of concentration in the centrifuged liquor, which is not reciprocated in the bulk. Thus, the difference in concentration between the two liquor fractions increases over time.

Then, after 60 min of cook, the rate of dissolution starts to decrease (refer to Figure 1A). In addition, the changes in the wood chip microstructure (e.g., separation of cell walls, formation of cracks, changes in cell wall thickness, etc.) possibly increased the transport rates of lignin fragments from the cell wall towards the lumen, and from the lumen towards the bulk liquor. Ultimately, the dissolution rate seems to fall below the rate of transport of the lignin fragments, so that the concentration in the lumen decreases.

A similar behavior can be observed in Figure 2B, though, while the maximum concentration of lignin occurs after 60 min in the CL, it occurs already around 30 min for xylan. This profile implies an early dissolution of xylan, which is also seen in Figure 1B, as the xylan concentration in the pulp decreases faster than the lignin content, and reaches a final value after 60 min. Again, this result reinforces that most of

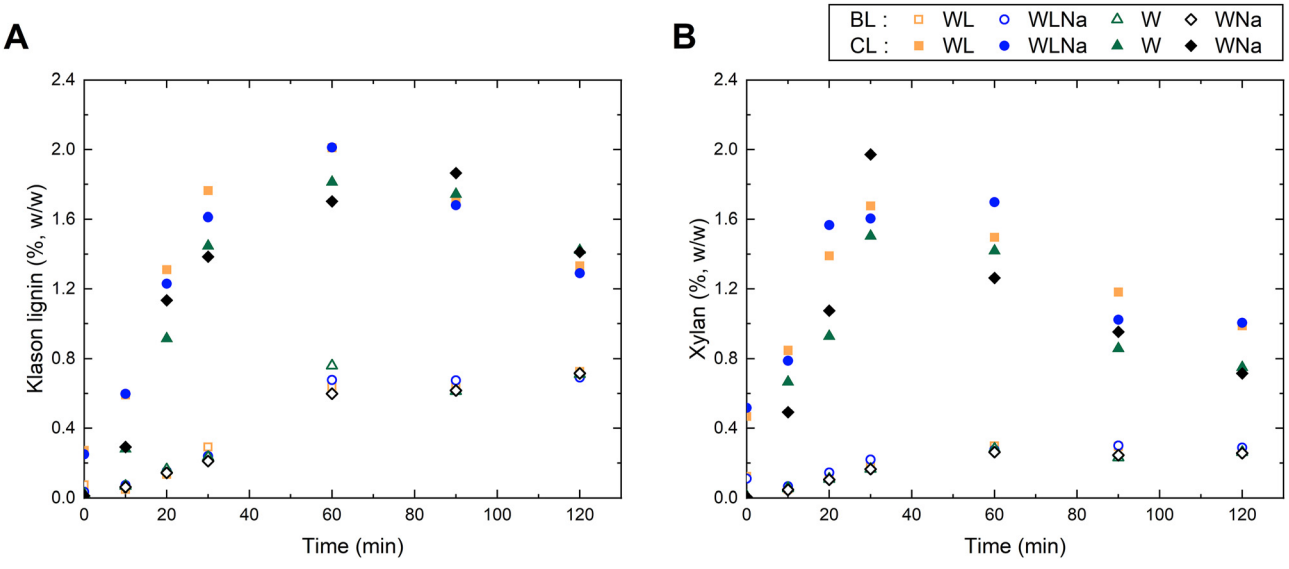

Figure 2: Content of Klason lignin (A) and xylan (B) in bulk (BL) and centrifuged (CL) liquor samples collected throughout cooking. Values at 0 min represent the composition of the spent impregnation liquor.

the xylan is removed during the heating up period, which is likely due to dissolution and, to a moderate extent, peeling. After 30 min, the xylan content in the CL decreases abruptly, which is explained by the transport from lumen to bulk, although xylan redeposition and degradation cannot be completely ruled out.

3.4 Composition of the precipitated lignin

To assess further differences between the two liquor fractions, lignin was precipitated from the centrifuged and bulk liquors originated from samples impregnated with liquor WL and cooked for either 30 or 90 min. The two time points were selected to represent early and late delignification, and to reflect the accumulating and decreasing phases of the lignin concentration in the CL fraction, as seen in Figure 2A. A compositional analysis was made, and the results are presented in Table 3. As expected, besides lignin, a large portion of the precipitated material consists of coprecipitated carbohydrates (mainly xylan). It is also worth noting that the percentage of lignin in the precipitated material increases over time and is larger in the bulk fraction. This is in line with the relative contents of lignin and xylan in the different liquid fractions: In CL 30, lignin and xylan are of approximately equal concentration, whereas in BL 90 the lignin concentration is more than twice as high as that of xylan. Additionally, the dissolved carbohydrates in the bulk liquor are likely more degraded than in the lumen, and thus are less likely to coprecipitate in polymeric form.

Table 3: Composition (%, w/w) of the precipitated material from bulk (BL) and centrifuged (CL) liquor.

Component	BL 30 min	BL 90 min	CL 30 min	CL 90 min
Klason lignin	51.2 ± 0.3	55.8 ± 0.8	46.7 ± 0.5	52.0 ± 0.7
ASL	10.5 ± 0.2	13.7 ± 1.4	12.8 ± 0.7	11.9 ± 0.3
Carbohydrates	28.7 ± 0.3	23.2 ± 0.1	34.4 ± 1.8	27.8 ± 0.2
Glucan	0.4 ± 0.0	0.3 ± 0.0	0.3 ± 0.0	0.4 ± 0.0
Xylan	28.3 ± 0.3	22.7 ± 0.1	34.2 ± 1.8	26.3 ± 0.2
Total	90.4 ± 0.5	92.7 ± 1.6	93.9 ± 2.0	91.7 ± 0.8

Reported values: $\bar{x} \pm s$.

3.5 Molecular weight of the precipitated lignin

The precipitated lignin samples were also analyzed for their molecular weight distribution (MWD). The UV detected distribution from the GPC is shown in Figure 3A. Lignin precipitated from the bulk liquor collected after 90 min had an MWD shifted towards a lower weight, when compared to the BL 30 min sample. However, studies using flow-through reactors show that the molecular weight (Mw) of dissolved lignin from both pine (Dang et al. 2016; Sjöholm et al. 1999b) and birch (Sjöholm et al. 1999a) increases over time during pulping. Thus, the decrease in molecular weight observed in the present study is most likely a direct result of employing a batch process, as the dissolved lignin was subjected to further degradation in the bulk prior to sampling. Nevertheless, previous research found this decrease to take place after reaching higher H-factors than those achieved here (Brännvall and Rönnols 2021; Pakkanen and Alén 2012), although the low wood:liquor ratio (and, consequently, lower residual alkali) applied in these studies may explain the different behaviors.

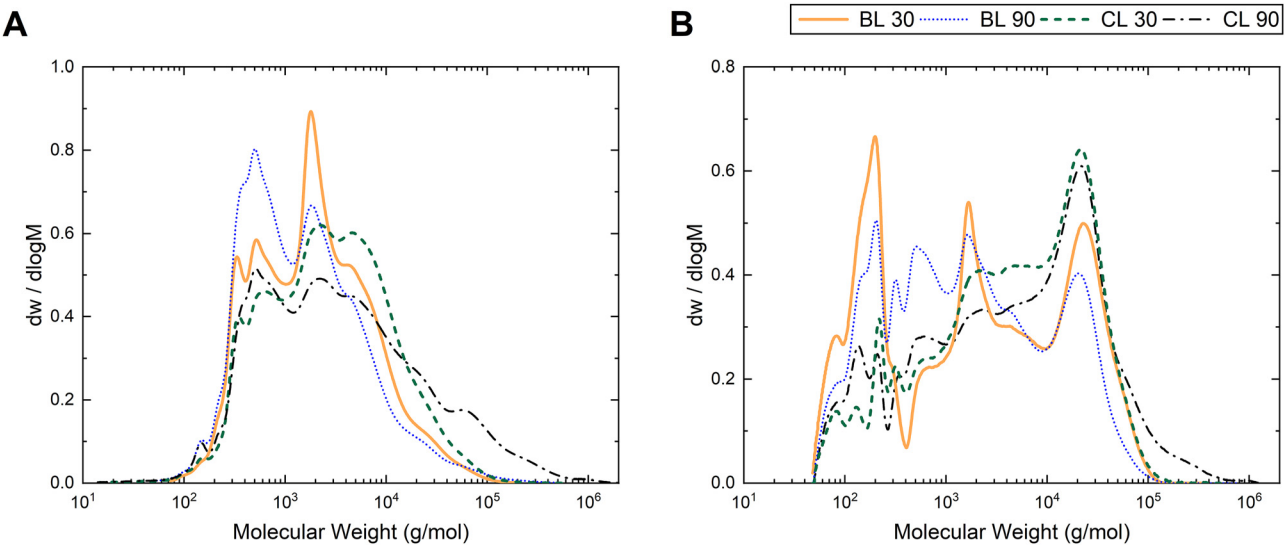

Figure 3: Differential molecular weight distribution of precipitated lignin from bulk (BL) and centrifuged (CL) liquors, sampled after 30 and 90 min, based on UV (A) and RI (B) detection.

For lignin precipitated from the centrifuged liquor, the weight distribution instead shifted towards higher molecular weights after 90 min, compared to 30 min. With time, lignin fragments of higher molecular weight, which diffuse more slowly, had time to be transferred out of the cell wall and into the lumen. Thus, this shift in molecular weight suggests a considerable transport resistance in the cell wall.

Finally, when comparing the MWD of lignin in bulk and centrifuged liquors, the latter showed a larger fraction of high molecular weight lignin. Interestingly, the increase over time of high molecular weight (Mw) fragments (>10 kDa) seen in the CL is not reciprocated in the BL. This could be the result of either (or both) effects discussed above: smaller lignin fragments are transported more quickly out into the bulk, and while out in the bulk, the access to an excess of active cooking chemicals results in continued fragmentation.

Compared to UV signals, the RI data also include responses from carbohydrates. Figure 3B presents the integrated RI response from the same data as presented in Figure 3A. The UV data showed the majority of peaks to fall in the range of 0.25–10 kDa, whereas the RI data in Figure 3B also show major peaks around 0.1–0.25 and 10–50 kDa. Consequently, the carbohydrates detected in the compositional analysis of the precipitated lignin stems from both dissolved monomers (detected in the low Mw range) and coprecipitated polymers (detected in the later high Mw range).

Likewise, the RI data exhibit the same trends as seen above: the centrifuged fractions contain more polymers with high Mw than the bulk, and the content of especially large molecules (>40 kDa) increases with time in the centrifuged fraction. Additionally, the proportion of carbohydrates with high molar mass decreases over time in the bulk, which again implies that extensive degradation has occurred.

3.6 NMR analysis of the precipitated lignin

The aliphatic inter-unit linkage region (δ_C/δ_H 50–90/3.5–5.5) of the HSQC spectra is shown in Figure 4. Assignment of selected peaks based on literature data is presented in Table 4 (Kim and Ralph 2014; Rencoret et al. 2009; Teleman et al. 1995; Yuan et al. 2011). Notably, signals assigned to the C_α in β-O-4

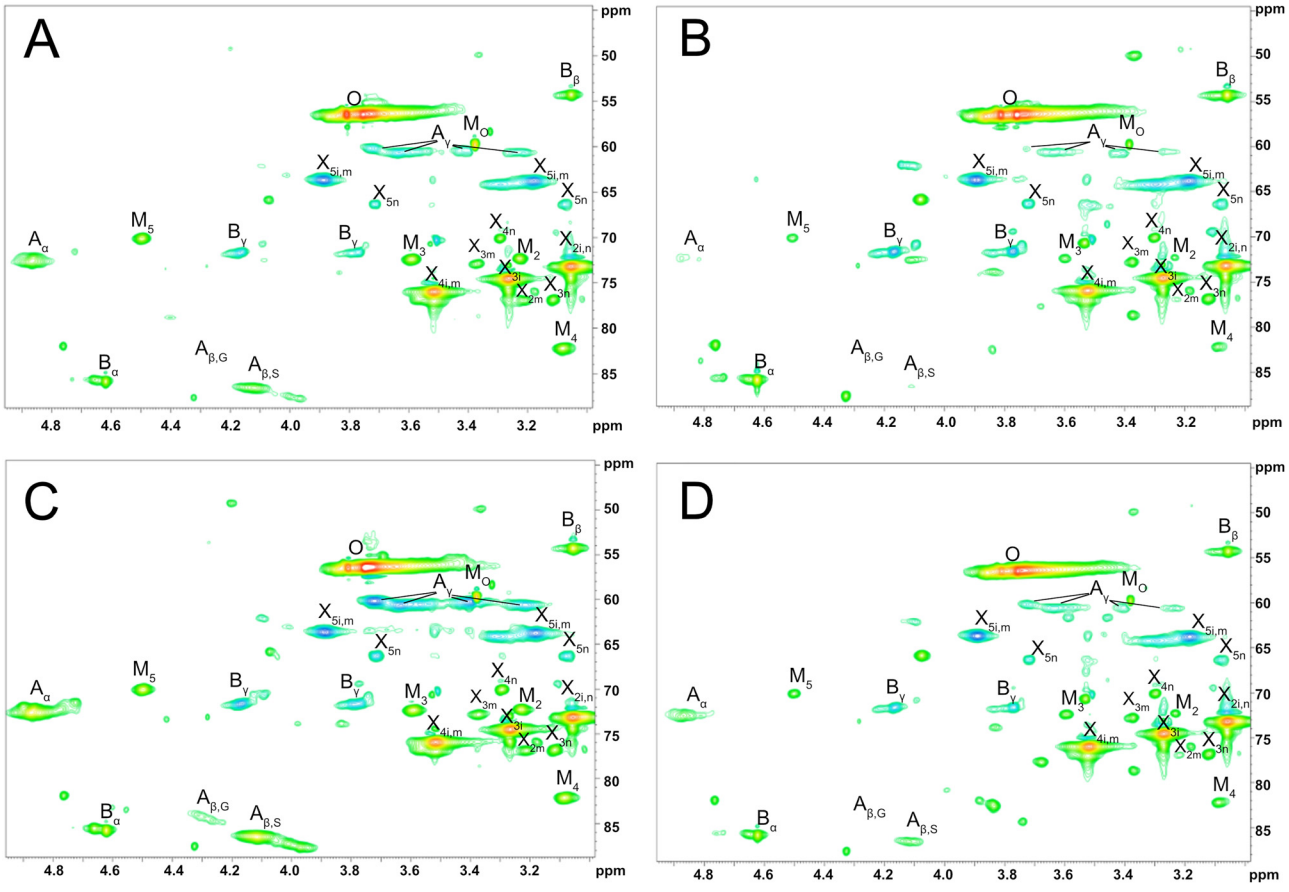

Figure 4: The aliphatic inter-unit and non-anomeric carbohydrate region (δ_C/δ_H 50–90/3.5–5.5 ppm) of the 2D NMR spectra for precipitated lignin samples from bulk liquor after 30 min (A) and after 90 min (B) of cook, and from centrifuged liquor after 30 min (C) and after 90 min (D). Annotated peaks are detailed in Table 4.

Table 4: Assigned peaks in the HSQC NMR data for lignin and polysaccharide structures in the precipitated material (solvent: DMSO-d_6).

Symbol	Structure	$^{13}C/^{1}H$ chemical shifts (ppm)
A_γ	C_γ–H_γ in β-O-4 structure	59.5–59.7/3.4–3.63
A_α	C_α–H_α in β-O-4 structure	71.8/4.86
$A_{\beta,G}$	C_β–H_β in β-O-4 with guaiacyl units	83.9/4.29
$A_{\beta,S}$	C_β–H_β in β-O-4 with syringyl units	85.9/4.12
B_β	C_β–H_β in resinol structure	54.2/3.06
B_γ	C_γ–H_γ in resinol structure	71.6/3.77 & 4.16
B_α	C_α–H_α in resinol structure	85.8/4.62
G_2	C_2–H_2 in guaiacyl unit	111.5/6.99
G_6	C_6–H_6 in guaiacyl unit	119.5/6.83
G_5	C_5–H_5 in guaiacyl unit	115.2/6.71 & 6.94
$S_{2,6}$	$C_{2,6}$–$H_{2,6}$ in syringyl unit	103.8/6.71
$S'_{2,6}$	$C_{2,6}$–$H_{2,6}$ in C_α-oxidized syringyl unit	106.7/7.03 & 7.23
O	C–H in methoxyls	56.4/3.74
M_O	C–H in MGA[a] (–OCH_3)	59.8/3.38
M_5	C_5–H_5 in MGA[a]	70.1/4.50
M_2	C_2–H_2 in MGA[a]	72.3/3.23
M_3	C_3–H_3 in MGA[a]	72.4/3.59
M_4	C_4–H_4 in MGA[a]	82.30/3.09
M_1	C_1–H_1 in MGA[a]	97.8/5.10
X_{5i}	C_5–H_5 in xylan (internal)	63.7/3.18 & 3.89
X_{2i}	C_2–H_2 in xylan (internal)	73.2/3.06
X_{3i}	C_3–H_3 in xylan (internal)	74.6/3.27
X_{4i}	C_4–H_4 in xylan (internal)	76.0/3.52
X_{1i}	C_1–H_1 in xylan (internal)	102.2/4.28
X_{5n}	C_5–H_5 in xylan (non-reducing end)	66.3/3.08 & 3.72
X_{4n}	C_4–H_4 in xylan (non-reducing end)	70.0/3.30
X_{2n}	C_2–H_2 in xylan (non-reducing end)	73.2/3.06
X_{3n}	C_3–H_3 in xylan (non-reducing end)	76.8/3.12
X_{1n}	C_1–H_1 in xylan (non-reducing end)	102.2/4.28
X_{5m}	C_5–H_5 in xylan (MGA)	63.7/3.18 & 3.89
X_{2m}	C_2–H_2 in xylan (MGA)	76.9/3.22
X_{3m}	C_3–H_3 in xylan (MGA)	72.8/3.37
X_{4m}	C_4–H_4 in xylan (MGA)	76.0/3.52
X_{1m}	C_1–H_1 in xylan (MGA)	101.7/4.50
Hex_1	C_1–H_1 in hexenuronic acid	98.6/5.24

[a]4-*O*-methyl-α-D-glucuronic acid (MGA).

structures were completely missing in the BL after 90 min, and corresponding C_γ signals were weaker compared to the other samples. The chemical shift of the signal from C_β in β-O-4 depends on if the ether bond is connected to a syringyl or guaiacyl subunit. Neither sample showed any signal for guaiacyl, whereas the syringyl peak was missing in the BL 90 sample. These observations suggest that some syringyl β-O-4 bonds were still intact in the dissolved lignin inside the lumen of the wood chips, even after 90 min. However, as lignin was transported out of the wood chip, and especially as it reached the bulk liquor with a high availability of cooking chemicals, it continued to fragment (thus the absence of peaks in the BL 90 sample), which agrees with the MWD results. Moreover, signals of resinol structures formed by β–β′ bonds existed in all analyzed spectra, but neither sample showed signals corresponding to β-5 bonds.

Still in the aliphatic region, it is possible to assess the carbohydrates' non-anomeric peaks. All samples showed signals related to 4-*O*-methyl-α-D-glucuronic acid (MGA) and xylan, including internal units (MGA substituted and unsubstituted) and non-reducing ends. There were no peaks usually associated with acetylated structures or lignin-carbohydrate complex linkages. These results indicate that a significant portion of the carbohydrates that coprecipitated with the lignin samples was, in fact, dissolved xylan. Moreover, as the xylan peaks were detected in all samples (regardless of the liquor fraction or cooking time), it is likely that the xylan chains were dissolved from the wood chips early on, even at low temperatures, which supports the observations made when discussing the decrease in xylan content in the pulp. In addition, xylan is known to be relatively resistant to alkaline conditions, which explains its presence as polysaccharide, even in the BL samples collected after 90 min, as also seen in the MWD from RI measurements (refer to Figure 3B).

Further analysis of the carbohydrates' non-anomeric region shows that samples treated for 90 min have additional peaks and lower intensity of the MGA signals. The less intense MGA peaks can be explained by the degradation of the group with increasing cooking time. Similarly, while it was not possible to assign the additional peaks, it is likely that they are associated with the conversion products of MGA or minor wood components, which were transported out of the cell wall throughout the cook.

The carbohydrates' anomeric region (δ_C/δ_H 90–105/3.5–6.0) of the HSQC spectra is shown in Figure 5. Three main signals were assigned: the C_1 in substituted xylan, the C_1 in unsubstituted xylan (for both internal and non-reducing end units) and the C_1 in MGA. Additionally, just as observed in the non-anomeric region, there were extra peaks detected in the samples treated for 90 min and the MGA peak lost intensity, corroborating the hypothesis of MGA conversion/degradation over time. The increase in intensity of the chemical shift at δ_C/δ_H 98.6/5.24, for example, could indicate the conversion of MGA to hexenuronic acid, which has also been observed in previous studies (Lisboa et al. 2005).

The aromatic region (δ_C/δ_H 100–130/5.5–8.5) of the HSQC spectra is shown in Figure 6. The two fractions taken after 90 min show a higher concentration of C_α-oxidized syringyl

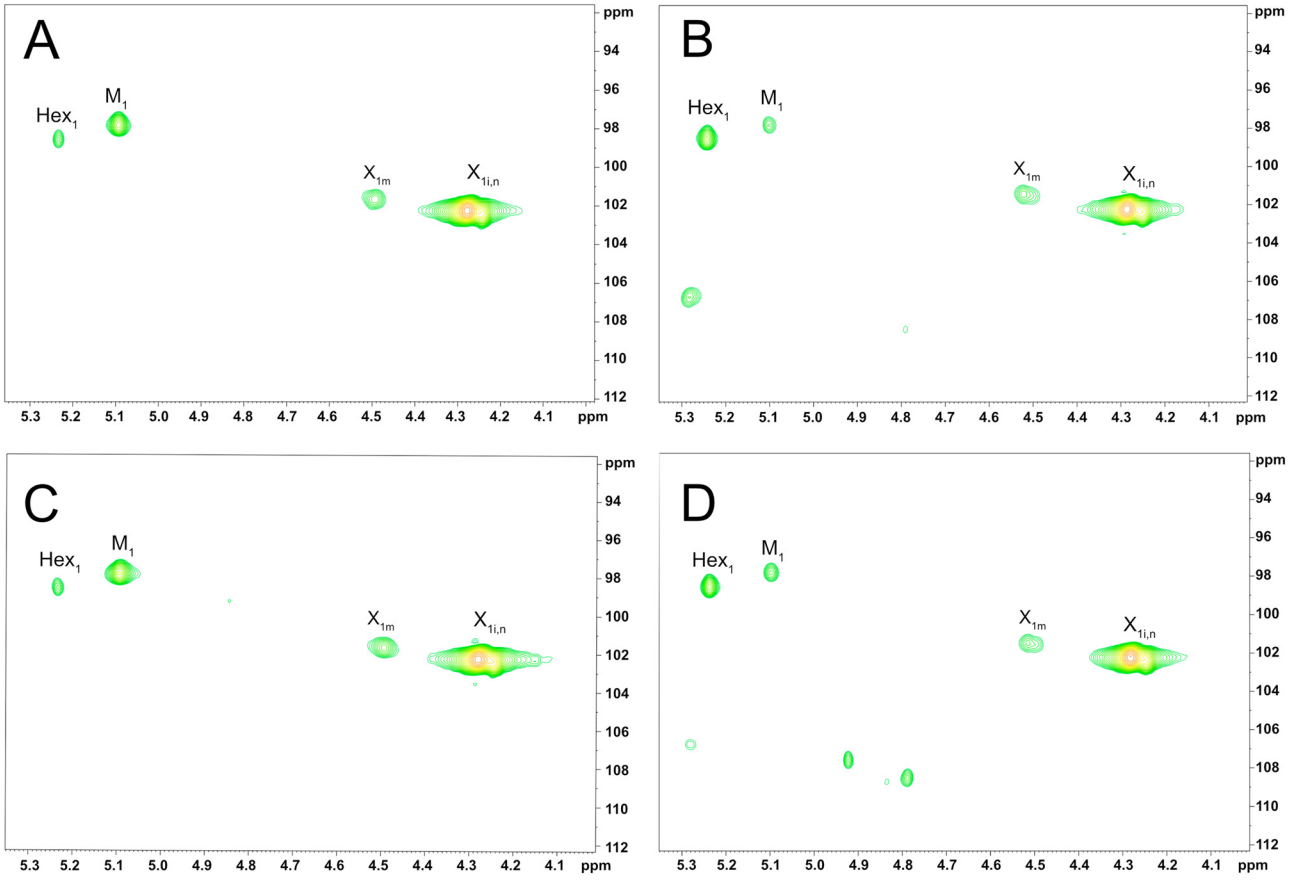

Figure 5: The anomeric carbohydrate region (δ_C/δ_H 90-105/3.5-6.0 ppm) of the 2D NMR spectra for precipitated lignin samples from bulk liquor after 30 min (A) and after 90 min (B) of cook, and from centrifuged liquor after 30 min (C) and after 90 min (D). Annotated peaks are detailed in Table 4.

units, whereas the two 30 min fractions show a stronger signal at the unmodified syringyl peak. This is especially evident for the CL30 sample, suggesting a less modified, and hence, more recently dissolved lignin.

Lastly, the C_2 and C_6 peaks of guaiacyl were found in the early samples, however, surprisingly, they disappear completely in the latter ones. The reason is unclear, as especially the C_2 position is generally seen as rather stable, and condensation products are mainly attributed to covalent linkages at the 5 position (Chiang et al. 1990). Although, similar findings of decreasing aromatic peaks have been reported (Balakshin and Capanema 2015). A possible explanation is the formation of 4-O-5 condensed structures, which will upfield-shift the C_2 signal of guaiacyl, which could explain the peak found at δ_C/δ_H 109.8/6.99 (Balakshin et al. 2003). As condensation reactions are known to increase towards the end of delignification, this reasonably explains why the uncondensed C_2 is missing only in the 90 min samples. However, condensation reactions could also occur during the acid precipitation step, hence further investigations are required.

4 Conclusions

The presence of active ions during impregnation increases the overall rate of delignification and carbohydrate degradation/dissolution during cooking, even under the mild impregnation conditions used in this study. In addition, there are significant limitations regarding the transport of dissolved wood components and degradation products from the lumen towards the bulk, regardless of the impregnation liquor applied. The lumen liquor was shown to have higher concentrations of lignin and xylan than the bulk, and the differences in the concentration profiles throughout cooking also reveal the effects of the transport resistance in the cell wall.

Further evidence of transport resistance is given by the increased concentration of high molecular weight material in the lumen compared to the bulk, which becomes even more pronounced as the cooking time increases. Moreover, a more severe degradation of lignin and carbohydrates is observed in the bulk liquor and/or with increasing cooking time, which was confirmed with NMR data showing a more

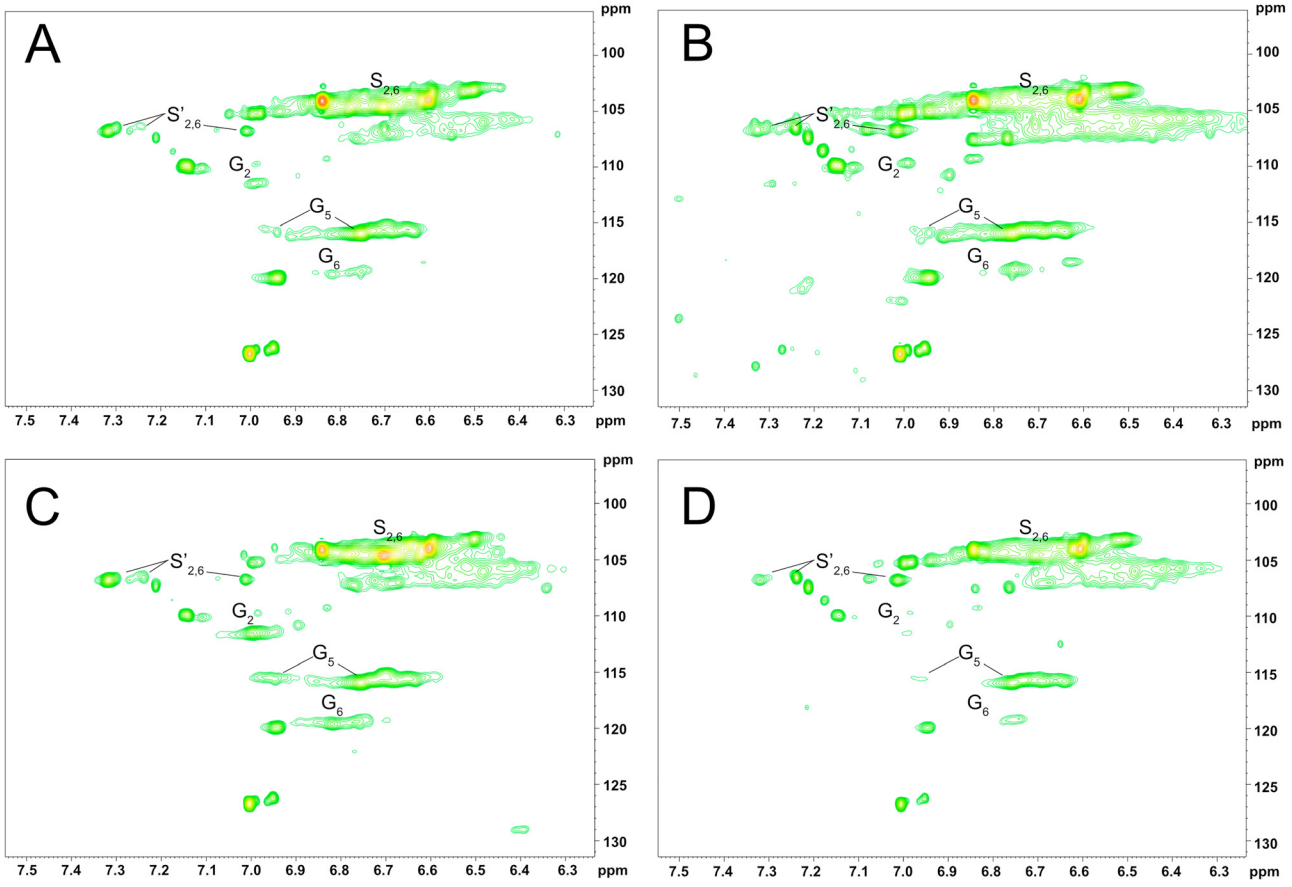

Figure 6: The aromatic region (δ_C/δ_H 100-130/5.5-8.5 ppm) of the 2D NMR spectra for precipitated lignin samples from bulk liquor after 30 min (A) and after 90 min (B) of cook, and from centrifuged liquor after 30 min (C) and after 90 min (D). Annotated peaks are detailed in Table 4.

pronounced cleavage of lignin inter-unit linkages and formation of degradation/conversion products.

In conclusion, there is clear evidence that both the molecular weight and the composition of the dissolved material differs between the bulk and pore liquor fractions. Therefore, it seems reasonable to consider the condition inside the wood chips (i.e., in cell wall and in lumen), and not only in the bulk liquor, when studying or modelling delignification kinetics.

Acknowledgments: The authors would like to thank Södra Skogsägarna for supplying the raw material used in this study, the Swedish NMR centre for providing time at the spectrometer, and Cara Boccieri for the linguistic review. The work was performed within the strategical innovation program BioInnovation – a joint initiative by Vinnova (Sweden's innovation agency), Formas (Swedish governmental research council for sustainable development) and the Swedish Energy Agency.

Author contributions: All the authors have accepted responsibility for the entire content of this article and agreed on its submission for publication.

Research funding: Collaboration and financial support of the Resource-smart Processes network financed by Vinnova via BioInnovation and industrial partners (Billerud, Holmen, SCA, Stora Enso, Södra Skogsägarna and Valmet) are gratefully acknowledged.

Conflict of interest statement: The authors declare that they have no conflicts of interest regarding this article.

References

Axelsson, S., Croon, I., and Enström, B. (1962). Dissolution of hemicelluloses during sulphate pulping. Sven. Papperstidning 18: 693–697.

Balakshin, M.Y. and Capanema, E.A. (2015). Comprehensive structural analysis of biorefinery lignins with a quantitative ^{13}C NMR approach. RSC Adv. 5: 87187–87199.

Balakshin, M.Y., Capanema, E.A., Chen, C.L., and Gracz, H.S. (2003). Elucidation of the structures of residual and dissolved pine kraft

lignins using an HMQC NMR technique. J. Agric. Food Chem. 51: 6116–6127.

Bijok, N., Fiskari, J., Gustafson, R.R., and Alopaeus, V. (2022). Modelling the kraft pulping process on a fibre scale by considering the intrinsic heterogeneous nature of the lignocellulosic feedstock. Chem. Eng. J. 438: 135548.

Bogren, J. (2008). *Further insights into kraft cooking kinetics*, Ph.D. thesis. Gothenburg, Chalmers University of Technology.

Bogren, J., Brelid, H., Bialik, M., and Theliander, H. (2009). Impact of dissolved sodium salts on kraft cooking reactions. Holzforschung 63: 226–231.

Brännvall, E. and Rönnols, J. (2021). Analysis of entrapped and free liquor to gain new insights into kraft pulping. Cellulose 28: 2403–2418.

Brelid, H., Bogren, J., Dang, B., Lundqvist, F., Saltberg, A., and Theliander, H. (2011). Kraft delignification: recent findings regarding the impact of non-reacting ions in the cooking liquor. In: *2011 TAPPI PEERS Conference*, pp. 717–739.

Chakar, F.S. and Ragauskas, A.J. (2004). Review of current and future softwood kraft lignin process chemistry. Ind. Crops Prod. 20: 131–141.

Chiang, V.L., Funaoka, M., and Products, W. (1990). The dissolution and condensation reactions of guaiacyl and syringyl units in residual lignin during kraft delignification of sweetgum. Holzforschung 44: 147–155.

Dammström, S., Salmén, L., and Gatenholm, P. (2009). On the interactions between cellulose and xylan, a biomimetic simulation of the hardwood cell wall. BioResources 4: 3–14.

Dang, B.T.T., Brelid, H., Köhnke, T., and Theliander, H. (2013). Impact of ionic strength on delignification and hemicellulose removal during kraft cooking in a small-scale flow-through reactor. Nordic Pulp Pap. Res. J. 28: 358–365.

Dang, B.T.T., Brelid, H., and Theliander, H. (2016). The impact of ionic strength on the molecular weight distribution (MWD) of lignin dissolved during softwood kraft cooking in a flow-through reactor. Holzforschung 70: 495–501.

Dang, V.Q. and Nguyen, K.L. (2008). A universal kinetic model for characterisation of the effect of chip thickness on kraft pulping. Bioresour. Technol. 99: 1486–1490.

Dence, C.W. (1992). The determination of lignin. In: Lin, S.Y. and Dence, C.W. (Eds.). *Methods in lignin chemistry. Springer Series in Wood Science*. Springer, Berlin, pp. 33–61.

Forest Europe (2020). *Adaptation to climate change in sustainable forest management in Europe*. Zvolen.

Gellerstedt, G., Majtnerova, A., and Zhang, L. (2004). Towards a new concept of lignin condensation in kraft pulping. Initial results. Comptes Rendus Biol. 327: 817–826.

Gierer, J. (1980). Chemical aspects of kraft pulping. Wood Sci. Technol. 14: 241–266.

Gilbert, W., Allison, B., Radiotis, T., and Dort, A. (2021). A simplified kinetic model for modern cooking of aspen chips. Nordic Pulp Pap. Res. J. 36: 399–413.

Grénman, H., Wärnå, J., Mikkola, J.P., Sifontes, V., Fardim, P., Murzin, D.Y., and Salmi, T. (2010). Modeling the influence of wood anisotropy and internal diffusion on delignification kinetics. Ind. Eng. Chem. Res. 49: 9703–9711.

Hatton, J.V. (1973). Development of yield prediction equations in kraft pulping. Tappi 56: 97–100.

Henriksson, G., Lawoko, M., Martin, M.E.E., and Gellerstedt, G. (2007). Lignin-carbohydrate network in wood and pulps: a determinant for reactivity. Holzforschung 61: 668–674.

Janson, J. (1974). Analytik der Polysaccharide in Holz und Zellstoff. Faserforschung und Textiltechnik 25: 375–382.

Kim, H. and Ralph, J. (2014). A gel-state 2D-NMR method for plant cell wall profiling and analysis: a model study with the amorphous cellulose and xylan from ball-milled cotton linters. RSC Adv. 4: 7549–7560.

Lindgren, C.T. and Lindström, M.E. (1996). The kinetics of residual delignification and factors affecting the amount of residual lignin during kraft pulping. J. Pulp Pap. Sci. 22: 290–295.

Lisboa, S.A., Evtuguin, D.V., Pascoal Neto, C., and Goodfellow, B.J. (2005). Isolation and structural characterization of polysaccharides dissolved in *Eucalyptus globulus* kraft black liquors. Carbohydr. Polym. 60: 77–85.

Luostarinen, K. and Hakkarainen, K. (2019). Chemical composition of wood and its connection with wood anatomy in *Betula pubescens*. Scand. J. For. Res. 34: 577–584.

Mattsson, C., Hasani, M., Dang, B., Mayzel, M., and Theliander, H. (2017). About structural changes of lignin during kraft cooking and the kinetics of delignification. Holzforschung 71: 545–553.

Mortha, G., Sarkanen, K., and Gustafson, R. (1992). Alkaline pulping kinetics of short-rotation, intensively cultured hybrid poplar. TAPPI J. 75: 99–104.

Mulat, D.G., Huerta, S.G., Kalyani, D., and Horn, S.J. (2018). Enhancing methane production from lignocellulosic biomass by combined steam-explosion pretreatment and bioaugmentation with cellulolytic bacterium Caldicellulosiruptor bescii. Biotechnol. Biofuels 11: 1–15.

Nguyen, K.L. and Dang, V.Q. (2006). The fractal nature of kraft pulping kinetics applied to thin *Eucalyptus nitens* chips. Carbohydr. Polym. 64: 104–111.

Nieminen, K. and Sixta, H. (2012). Comparative evaluation of different kinetic models for batch cooking: a review. Holzforschung 66: 791–799.

Olm, L., Tormund, D., and Lundqvist, F. (2009). High sulphidity kraft pulping. Nordic Pulp Pap. Res. J. 24: 433–439.

Pakkanen, H. and Alén, R. (2012). Molecular mass distribution of lignin from the alkaline pulping of hardwood, softwood, and wheat straw. J. Wood Chem. Technol. 32: 279–293.

Pätäri, S., Tuppura, A., Toppinen, A., and Korhonen, J. (2016). Global sustainability megaforces in shaping the future of the European pulp and paper industry towards a bioeconomy. For. Pol. Econ. 66: 38–46.

Pinto, P.C., Evtuguin, D.V., and Neto, C.P. (2005). Effect of structural features of wood biopolymers on hardwood pulping and bleaching performance. Ind. Eng. Chem. Res. 44: 9777–9784.

Rahman, M., Avelin, A., and Kyprianidis, K. (2020). A review on the modeling, control and diagnostics of continuous pulp digesters. Processes 8: 1231.

Rencoret, J., Marques, G., Gutiérrez, A., Nieto, L., Santos, J.I., Jiménez-Barbero, J., Martínez, Á.T., and Del Río, J.C. (2009). HSQC-NMR analysis of lignin in woody (Eucalyptus globulus and Picea abies) and non-woody (Agave sisalana) ball-milled plant materials at the gel state. Holzforschung 63: 691–698.

Ruel, K., Chevalier-billosta, V., Guittemin, F., Sierra, J.B., and Joseleau, J.P. (2006). The wood cell wall at the ultrastructural scale formation and topochemical organization. Maderas Cienc. Tecnol. 8: 107–116.

Saltberg, A., Brelid, H., and Lundqvist, F. (2009). The effect of calcium on kraft delignification – study of aspen, birch and eucalyptus. Nordic Pulp Pap. Res. J. 24: 440–447.

Santos, R.B., Capanema, E.A., Balakshin, M.Y., Chang, H.M., and Jameel, H. (2011). Effect of hardwoods characteristics on kraft pulping process: emphasis on lignin structure. BioResources 6: 3623–3637.

Santos, R.B., Jameel, H., Chang, H.M., and Hart, P.W. (2012). Kinetics of hardwood carbohydrate degradation during kraft pulp cooking. Ind. Eng. Chem. Res. 51: 12192–12198.

Santos, R.B., Hart, P.W., Jameel, H., and Chang, H.-M. (2013). Important reactions of lignin. BioResources 8: 1456–1477.

Shin, S.J., Schroeder, L.R., and Lai, Y.Z. (2004). Impact of residual extractives on lignin determination in kraft pulps. J. Wood Chem. Technol. 24: 139–151.

Simão, J.P.F., Egas, A.P.V., Carvalho, M.G., Baptista, C.M.S.G., and Castro, J.A.A.M. (2008). Heterogeneous studies in pulping of wood: modelling mass transfer of alkali. Chem. Eng. J. 139: 615–621.

Simão, J.P.F., Carvalho, M.G.V.S., and Baptista, C.M.S.G. (2011). Heterogeneous studies in pulping of wood: modelling mass transfer of dissolved lignin. Chem. Eng. J. 170: 264–269.

Sixta, H. and Rutkowska, E.W. (2006). Modelling of *Eucalyptus globulus* kraft pulping. In: *Workshop on chemical pulping processes*.

Sjöholm, E., Gustafsson, K., and Colmsjö, A. (1999a). Size exclusion chromatography of lignins using lithium chloride/ N,N-dimethylacetamide as mobile phase. I. Dissolved and residual birch kraft lignins. J. Liq. Chromatogr. Relat. Technol. 22: 1663–1685.

Sjöholm, E., Gustafsson, K., and Colmsjö, A. (1999b). Size exclusion chromatography of lignins using lithium chloride/ N,N-dimethylacetamide as mobile phase. II. Dissolved and residual pine kraft lignins. J. Liq. Chromatogr. Relat. Technol. 22: 2837–2854.

Sjöström, E. (1977). The behavior of wood polysaccharides during alkaline pulping processes. Tappi 60: 151–154.

Sluiter, A., Hames, B., Ruiz, R., Scarlata, C., Sluiter, J., Templeton, D., Crocker, D. (2012). Determination of structural carbohydrates and lignin in biomass – NREL/TP-510-42618. Laboratory Analytical Procedure (LAP) 17.

Tavast, D. and Brännvall, E. (2017). Increased pulp yield by prolonged impregnation in softwood kraft pulping. Nordic Pulp Pap. Res. J. 32: 14–20.

Teleman, A., Harjunpää, V., Tenkanen, M., Buchert, J., Hausalo, T., Drakenberg, T., and Vuorinen, T. (1995). Characterisation of 4-deoxy-β-l-threo-hex-4-enopyranosyluronic acid attached to xylan in pine kraft pulp and pulping liquor by 1H and 13C NMR spectroscopy. Carbohydr. Res. 272: 55–71.

Wojtasz-Mucha, J., Hasani, M., and Theliander, H. (2017). Hydrothermal pretreatment of wood by mild steam explosion and hot water extraction. Bioresour. Technol. 241: 120–126.

Yuan, T.Q., Sun, S.N., Xu, F., and Sun, R.C. (2011). Characterization of lignin structures and lignin-carbohydrate complex (LCC) linkages by quantitative 13C and 2D HSQC NMR spectroscopy. J. Agric. Food Chem. 59: 10604–10614.

Supplementary Material: This article contains supplementary material (https://doi.org/10.1515/hf-2023-0018).